# The NMR Structure of Cyclosporin A Bound to Cyclophilin in Aqueous Solution†

C. Weber,‡ G. Wider,‡ B. von Freyberg,‡ R. Traber,§ W. Braun,‡ H. Widmer,§ and K. Wüthrich*,‡

*Institut für Molekularbiologie und Biophysik, Eidgenössische Technische Hochschule—Hönggerberg, CH-8093 Zürich, Switzerland, and Präklinische Forschung, Sandoz Pharma AG, CH-4002 Basel, Switzerland*

*Received December 31, 1990; Revised Manuscript Received March 28, 1991*

ABSTRACT: Cyclosporin A bound to the presumed receptor protein cyclophilin was studied in aqueous solution at pH 6.0 by nuclear magnetic resonance spectroscopy using uniform $^{15}N$- or $^{13}C$-labeling of cyclosporin A and heteronuclear spectral editing techniques. Sequence-specific assignments were obtained for all but one of the cyclosporin A proton resonances. With an input of 108 intramolecular NOEs and four vicinal $^3J_{HN\alpha}$ coupling constants, the three-dimensional structure of cyclosporin A bound to cyclophilin was calculated with the distance geometry program DISMAN, and the structures resulting from 181 converged calculations were energy refined with the program FANTOM. A group of 120 conformers was selected on the basis of the residual constraint violations and energy criteria to represent the solution structure. The average of the pairwise root-mean-square distances calculated for the backbone atoms of the 120 structures was 0.58 Å. The structure represents a novel conformation of cyclosporin A, for which the backbone conformation is significantly different from the previously reported structures in single crystals and in chloroform solution. The structure has all peptide bonds in the trans form, contains no elements of regular secondary structure and no intramolecular hydrogen bonds, and exposes nearly all polar groups to its environment. The root-mean-square distance between the backbone atoms of the crystal structure of cyclosporin A and the mean of the 120 conformers representing the NMR structure of cyclosporin A bound to cyclophilin is 2.5 Å.

The immunosuppressive cyclic undecapeptide cyclosporin A (CsA)[1] (Figure 1) has found widespread use in clinical organ transplantation (Borel, 1986; Kahan, 1988). Much insight has been gained into its action on lymphoid cells at a subcellular level. Among other things it inhibits lymphokine production by T-helper cells on the level of mRNA transcription in vitro (Krönke et al., 1984; Elliot et al., 1984) by the inhibition of specific transcriptional activators, such as the nuclear factor of activated T-cells, NF-AT (Emmel et al., 1989). Relative to the molecular basis for its in vivo and in vitro properties, Handschumacher et al. (1984) have described the cytosolic binding protein cyclophilin and proposed that it is the cellular receptor. Cyclophilin (CYP) has been found in diverse organisms from *Escherichia coli* to man (Koletsky et al., 1986; Kawamukai et al., 1989), and in all tissues studied it is present at high abundance. Recently it was found that the enzyme peptidyl–prolyl cis–trans isomerase is identical with CYP (Fischer et al., 1989; Takahashi et al., 1989) and that CsA is a potent inhibitor ($K_i$ = 2.6 nM) of the enzymatic action. It was proposed that CsA exerts its effects on cells via the inhibition of the cis–trans isomerization. Harrison and Stein (1990) have presented elegant kinetic evidence for a mechanism based on distortion of the susceptible peptide bond.

Implications for the mode of interaction between CsA and CYP are so far based on indirect evidence. The structure of cyclosporin A in single crystals and in apolar solvents has been determined (Loosli et al., 1985; Kessler et al., 1990). In both environments it consists of a twisted $\beta$-sheet involving the residues 11, 1, 2, 3, 4, 5, 6, and 7, a type II′ turn at Sar 3 and MeLeu 4, and the loop of the remaining amino acids involves a cis peptide bond between MeLeu 9 and MeLeu 10. Monoclonal antibodies raised against CsA were used by Quesniaux and co-workers (Quesniaux et al., 1987a, 1988) to identify the recognition sites of CsA. They measured the cross reactivity of cyclosporin analogues modified at various positions and concluded that in aqueous solution the side chain of MeBmt 1 is folded back onto the molecule as in both the crystal structure and the structure in chloroform solution (Kessler et al., 1990), since antibodies recognizing the face of the molecule defined by the residues 6, 8, and 9 also recognize the peripheral atoms of the MeBmt side chain. These workers also investigated the ability of cyclosporin analogues to CYP using ELISA techniques. They found that recognition of cyclosporins by CYP correlates with the immunosuppressive activity and that CYP interacts preferentially with the residues 1, 2, 10, and 11 of cyclosporin A (Quesniaux et al., 1987b). To gain more direct insight into the molecular details of the function of CsA, we investigated its complex with CYP by nuclear magnetic resonance (NMR) spectroscopy in solution, making extensive use of heteronuclear editing techniques (Fesik, 1988; Fesik et al., 1988; Griffey & Redfield, 1987; Otting et al., 1986). In particular, the use of heteronuclear

† Financial support was obtained from the Schweizerischer Nationalfonds (project no. 31.25174.88), a special grant of the ETH Zürich, and Sandoz Pharma AG., Basel.

‡ Institut für Molekularbiologie and Biophysik.

§ Präklinische Forschung.

[1] Abbreviations: NMR, nuclear magnetic resonance; CYP, cyclophilin; CsA, cyclosporin A; MeBmt, (4*R*)-4-[(*E*)-2-butenyl]-4,*N*-dimethyl-L-threonine; Abu, L-$\alpha$-aminobutyric acid; MeLeu, *N*-methylleucine; MeVal, *N*-methylvaline; FAB-MS, fast atom bombardment mass spectrometry; hplc, high-performance liquid chromatography; Tris, tris(hydroxymethyl)aminomethane; PMSF, phenylmethanesulfonyl fluoride; EDTA, ethylenediaminetetraacetic acid; DTT, dithiothreitol; MES, 4-morpholineethanesulfonic acid; 1D, one dimensional; 2D, two dimensional; COSY, two-dimensional correlation spectroscopy; TOCSY, two-dimensional total correlation spectroscopy; NOE, nuclear Overhauser effect; NOESY, two-dimensional NOE spectroscopy; CD, circular dichroism; $d_{AB}(i,j)$ designates the distance between the proton types A and B located in the amino acid residues $i$ and $j$ respectively, where N, NQ, $\alpha$, and $\beta$ denote the amide proton, the N-methyl protons, $C^{\alpha}H$, and $C^{\beta}H$, respectively; RMSD, root-mean-square deviation.

0006-2960/91/0430-6563$02.50/0 

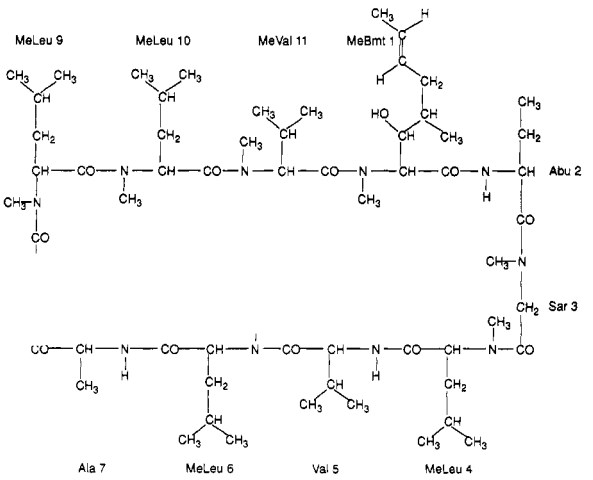


FIGURE 1: Chemical structure of cyclosporin A (CsA) with the standard numeration of the amino acid residues. Symbols: MeBmt, (4*R*)-4-[(*E*)-2-butenyl]-4,*N*-dimethyl-L-threonine; Abu, L-α-aminobutyric acid; MeLeu, *N*-methylleucine; MeVal, *N*-methylvaline.

filters (Otting & Wüthrich, 1990) in conjunction with uniform $^{15}N$ and $^{13}C$ enrichment of CsA enabled the spectroscopic distinction of the two molecules in the complex. 2D [$^1H$,$^1H$] NMR spectra recorded with a $^{13}C$ double half-filter (Otting & Wüthrich, 1989, 1990), were processed into four subspectra, of which one contains only resonances of CsA without interference from CYP, one contains only resonances of CYP without interference from CsA, and two contain exclusively peaks connecting protons of CsA with protons of CYP. For the present work the subspectrum containing the $^1H$ NMR lines of CsA was of most direct importance, as it enabled the use of the well-established protocol for sequential assignment of all CsA proton resonances and collection of a set of conformational constraints to derive a three-dimensional structure of CsA in the bound state (Wüthrich, 1986, 1989). Another study of CsA bound to CYP conducted independently by another group is described in the accompanying paper (Fesik et al., 1991).

## Material and Methods

*Preparation of Isotope-Labeled CsA.* Uniformly $^{15}N$-labeled CsA was obtained by growing a high-producing strain of *Tolypocladium inflatum* on a minimal medium consisting of unlabeled glucose (50 g/L), [$^{15}N$]urea (4 g/L, 99% $^{15}N$, Isotech Inc., Miamisburg, OH), and salts and vitamins as described by Kobel and Traber (1982). After 21 days of growth at 27 °C, with shaking at 200 rpm in 500-mL Erlenmeyer flasks, the mycelium was homogenized, extracted with 50% methanol, filtered through celite, and then the liquid phase was evaporated. The crude extract was chromatographed on silicagel, with 9:1 diethylether/methanol as the liquid phase, and the CsA-containing fractions (as judged by thin-layer chromatography) were pooled and analyzed by reverse-phase hplc and FAB-MS. The $^{15}N$-enriched CsA eluted as a single peak in reverse-peak hplc and accounted for >97% of the total integrated intensity. From the mass spectrum, we calculated that the $^{15}N$ enrichment was >98%. Uniformly $^{13}C$-labeled CsA was obtained with the same method, by utilizing [$^{13}C_6$]glucose (>98% $^{13}C$, Cambridge Isotope Lab., Woburn, MA) and unlabeled urea in an otherwise identical medium. The $^{13}C$-enriched CsA was >98% pure as analyzed by reverse-phase hplc. From the position and the width of the molecular ion peak in the mass spectrum, we calculated the $^{13}C$ enrichment to be >97%. In a control experiment in which the fungus was grown on unlabeled glucose and [$^{13}C$]urea, there was no evidence for $^{13}C$ enrichment, indicating that the carbon atom of urea is not used as a carbon source. Biosynthetically directed fractional $^{13}C$ labeling of CsA was obtained by growing the fungus on a mixture of 10% [$^{13}C_6$]glucose and 90% unlabeled glucose (Senn et al., 1989).

*Preparation of Recombinant Human CYP.* The protein was overexpressed in *E. coli*. The gene was cloned from Jurkat cells (Haendler et al., 1987) and was under control of a *Taq* promoter. The cells were grown to the stationary phase in a buffer containing casamino acids (25 g/L), yeast extract (10 g/L), and glucose (30 g/L), harvested by centrifugation, and stored at −40 °C. Frozen cells were thawed and suspended in two volumes of a buffer containing 25% sucrose, 50 mM Tris-HCl at pH 7.5, 2 mM EDTA, 1 mM PMSF, 1 mM *o*-phenanthroline, and 2.5 mg/mL lysozyme. After 4 h the solution was supplemented with 20 mg/L deoxyribonuclease I, 4 mg/L $MgCl_2$, 0.2 mg/L $MnCl_2$ and stirred. After 6–12 h at room temperature, the solution was centrifuged at 12000*g* for 40 min and the supernatant decanted. The pellet was resuspended in two volumes of extraction buffer and extracted as above. A total of 40–200 mL of the clear lysate was loaded onto 190 mL of Affi-Gel 10 (Bio-Rad, Richmond, CA) derivatized with 1,1-dihydro-*O*-acetyl-8-D-β-aminoalanine-cyclosporin (K. Stedman, personal communication). The column was eluted with 50 mM Tris-HCl, 2 mM EDTA, 2 mM DTT, pH 7.5, with a longitudinal flow of 0.2 cm/min. CYP eluted as an asymmetric shallow peak at 1100 mL. The UV-positive fractions were pooled and concentrated by ultrafiltration with an Amicon YM-10 membrane. The pooled fractions from the affinity column were diafiltered into 20 mM MES-NaOH, 2 mM EDTA, 2 mM DTT, pH 6.0. Up to 70 mg of CYP were loaded onto a Mono S HR 10-10 column (Pharmacia LKB, Uppsala, Sweden) equilibrated with the same buffer. The column was eluted with a gradient from 50 to 180 mM NaCl in the same buffer in two column volumes at a linear flow rate of 2.5 cm/min. As soon as UV-positive fractions appeared, the gradient was halted, and all CYP fractions eluted isocratically. The main CYP peak was cut at 30% peak height and stored at 4 °C. The main fractions of the previous step containing up to 150 mg of CYP in a volume of 3–10 mL were applied onto 450 mL of Sephacryl S-100 HR (Pharmacia LKB, Uppsala, Sweden) in a 2.6 × 84 cm column. The column was eluted with 20 mM MES-NaOH, 2 mM EDTA, 2 mM DTT, pH 6.0, at a flow rate of 0.2 cm/min. CYP eluted at 293 mL as a single peak, which was cut at 20% peak height. These fractions were sterile filtered and stored at 4 °C.

*NMR Samples of the CsA–CYP Complex.* The procedure used for the preparation of the complex was largely dictated by the fact that CsA is nearly insoluble in water. In a solution containing 10 mg of CYP, the aforementioned buffer was exchanged against either 99.8% $^2H_2O$ or a mixture of 90% $H_2O$/10% $D_2O$ containing 10 mM potassium deuteroacetate (Glaser AG, Basel, Switzerland) and 10 mM potassium phosphate at pH 6.0 (uncorrected pH meter reading). CsA was added from a 60 mg/mL stock solution in deuterated ethanol (99.5% $^2H$, Glaser AG, Basel, Switzerland) to a final CsA/CYP ratio of 2:1 by slow stepwise infusion through a very fine needle ensuring good dispersion of the resulting solid particles. The suspension was vortexed between subsequent additions of CsA and sonicated in the middle and at the end of the infusion procedure. The complexation was monitored by the disappearance of two methyl resonances at −0.57 and −0.14 ppm in the 1D $^1H$ NMR spectrum of free CYP and the concomitant appearance of two new methyl resonances at −0.90 and −0.69 ppm in the spectrum of the complex. Excess

solid CsA was removed by centrifugation and the supernatant twice diluted with 4 mL of the above buffer and concentrated to 500 μL in an Amicon Centriprep 10 ultrafiltration unit to lower the ethanol content. It was then transferred to an NMR tube. Two types of complexes were prepared: $^{15}$N-labeled CsA bound to CYP in $H_2O$ solution to study the amide protons of CsA and $^{13}$C-labeled CsA bound to CYP in $^2H_2O$ solution to study the carbon-bound protons of CsA.

*NMR Experiments.* $^{15}N(\omega_2)$ half-filtered and $^{13}C$-$(\omega_1,\omega_2)$-double-half-filtered 2D [$^1$H,$^1$H] NMR spectra were recorded with the previously described pulse sequences for COSY, TOCSY, and NOESY (Otting & Wüthrich, 1990) on Bruker AM-500 and AM-600 instruments at 25 °C. Data sets of 400 by 2048 points were acquired with sweep widths of 8064 Hz. The filter delays were set to 5.5 ms for $^{15}$N-filtered and 3.6 ms for $^{13}$C-filtered experiments. Heteronuclear decoupling was accomplished by a 180° proton pulse in the middle of $t_1$ and WALTZ decoupling in $t_2$. 90° pulse lengths were 10.5 μs for protons, 21 μs or 190 μs (for WALTZ decoupling) for $^{15}$N, and 13.2 μs or 85 μs (for WALTZ decoupling) for $^{13}$C. The transmitter was offset to 118 ppm in the $^{15}$N dimension and to 40 ppm in the $^{13}$C dimension. Heteronuclear correlation spectra were recorded with the pulse sequence of Bodenhausen and Ruben (1980) modified by addition of a spin lock purge pluse to suppress all signals originating from protons not bound to a heterospin (Otting & Wüthrich, 1988). No additional $H_2O$ suppression was needed in these experiments, and there was therefore no loss of NH resonance line intensity (Messerle et al., 1989). For [$^{13}$C,$^1$H]-COSY of CsA with biosynthetically directed fractional $^{13}$C labeling in the complex, the transmitter was offset to 28.5 ppm and the spectral width in the $^{13}$C dimension was reduced to 52 ppm. A NOE-relayed [$^{13}$C,$^1$H]-COSY experiment was recorded with a $^{13}C(\omega_2)$ half-filter. The resulting spectrum contains the same information as [$^1$H,$^1$H]-NOESY recorded with a $^{13}C(\omega_2,\omega_2)$ double half-filter, but it has the advantage that peaks that are overlapped in the latter experiment may be resolved along the $^{13}$C frequency axis (Wider et al., 1991). $^3J_{HN\alpha}$ coupling constants were determined with a 1D version of the *J*-modulated [$^{15}$N,$^1$H]-COSY experiment (Neri et al., 1990), which used $^{15}$N decoupling during acquisition and was acquired with 5632 transients per $\tau_2$ value. A total of 10 $\tau_2$ values with 10-ms intervals ranging from 0 to 90 ms were used, and the peak amplitudes were fitted to the expression

$$V(\tau_2) = A[\cos(\pi J\tau_2)\cos(\pi J\tau_1) - 0.5\sin(\pi J\tau_2)\sin(\pi J\tau_1)]e^{(-\tau_2/T_2)} \quad (1)$$

where $V(\tau_2)$ is the experimental peak amplitude, $A$ the peak amplitude at $\tau_2 = 0$, $J$ the coupling constant $^3J_{HN\alpha}$, and $T_2$ the transverse relaxation time (D. Neri, M. Billeter, G. Otting, G. Wider, and K. Wüthrich, to be published). The spectra were processed on Bruker Aspect 1000 or X32 computers using standard software, except for homemade software for the addition/subtraction operations.

*Determination of the Three-Dimensional CsA Structure.* For the collection of the conformational constraints, the NMR spectra were analyzed with the program package EASY (Eccles et al., 1989) on SUN computers. Three-dimensional structures of the bound form of CsA consistent with the NOE distance constraints and dihedral angle constraints were calculated by using the distance geometry program DISMAN (Braun & Gō, 1985). The nonstandard amino acids of CsA, i.e., MeBmt, Abu, Sar, MeLeu, and MeVal, were constructed with the program package GEOM (Sanner et al., 1989) and deposited into the library of DISMAN. Two open chain forms of CsA with Ala 7 at the amino terminal and MeLeu 6 at the carboxy terminal, or with MeBmt 1 at the amino terminal and MeVal 11 at the carboxy terminal, respectively, were assembled from the monomeric building blocks of the library. Conformations of the linear chain with random dihedral angles generated by DISMAN were used as starting structures for the distance geometry calculations. Geometric cyclization of the structures was achieved either with nine distance constraints between N, $C^\alpha$, and HN of Ala 7 and C, O, and $C^\alpha$ of MeLeu 6, or between N, $C^\alpha$, and QCN of MeBmt 1 and C, O, and $C^\alpha$ of MeVal 11. After cyclization, the ω angle of the C-terminal amino acid was thus fixed in the trans conformation. The program DISMAN was modified to selectively exclude repulsive van der Waals checks for cyclic structures (Senn et al., 1990). Method B in the previous structure determination of a cyclic bouvardin analogue (Senn et al., 1990) was used for the distance geometry calculations: the cyclization constraints and the experimental NOE constraints were used simultaneously. Structures with a final target function below a predetermined threshold value were retained and subjected to energy minimization using the program FANTOM (Schaumann et al., 1990), which had been adjusted for use with a cyclic peptide. FANTOM minimizes the ECEPP/2 energy function for proteins (Momany et al., 1975; Némethy et al., 1983) using a Newton–Raphson method. The torsion angles are the independent variables, and the ideal covalent geometry of ECEPP/2 is strictly retained during the minimization. Calculations were done on SUN4 and Cray X/MP computers. The resulting structures were graphically analyzed on an E&S PS 390 system using the program CONFOR (Billeter et al., 1985).

## Results

*Complex Formation between CYP and CsA.* CsA is very little soluble in $H_2O$, and therefore during the aforementioned procedure for the preparation of the complex with CYP the solution contains temporarily up to 5% ethanol (within 24 h after the preparation of the complex, the ethanol was removed by dialysis). Exploratory experiments using CD and 1D NMR spectroscopy revealed no evidence for conformational changes in cyclophilin, and measurements of the fluorescence enhancement of the single Trp in CYP upon binding of CsA showed that the CsA binding properties of CYP were not affected by the ethanol either. In the NMR samples, the concentration of the CYP–CsA complex was 0.8 mM, and because of the low solubility of CsA, there was no detectable concentration of free ligand. In the $^1$H NMR spectra of aqueous solutions containing an excess of CYP, two sets of resonance lines for free and complexed CYP were observed, showing that chemical exchange of the ligand is slow on the NMR chemical shift time scale.

*NMR Assignments for CsA Bound to CYP.* For studies of the conformation of a peptide ligand bound to a polypeptide receptor, obtaining $^1$H NMR assignments (Wüthrich et al., 1982; Wüthrich, 1986) is difficult because many $^1$H resonances of the ligand are overlapped with the much more numerous NMR lines originating from the receptor. Here, this difficulty was overcome by recording 2D [$^1$H,$^1$H] NMR spectra of complexes with isotope-labeled CsA and unlabeled CYP using heteronuclear half-filters (Fesik, 1988; Otting et al., 1986; Otting & Wüthrich, 1990). Figure 2 affords an illustration of the information contained in the subspectra that were most important for obtaining the resonance assignments. A $^{15}N(\omega_2)$-selected subspectrum from a [$^1$H,$^1$H]-NOESY experiment with an $^{15}N(\omega_2)$-half-filter (Otting et al., 1986) contains only the CsA amide proton lines along $\omega_2$ and all proton lines of CsA and CYP along $\omega_1$ so that all intra- and intermolecular

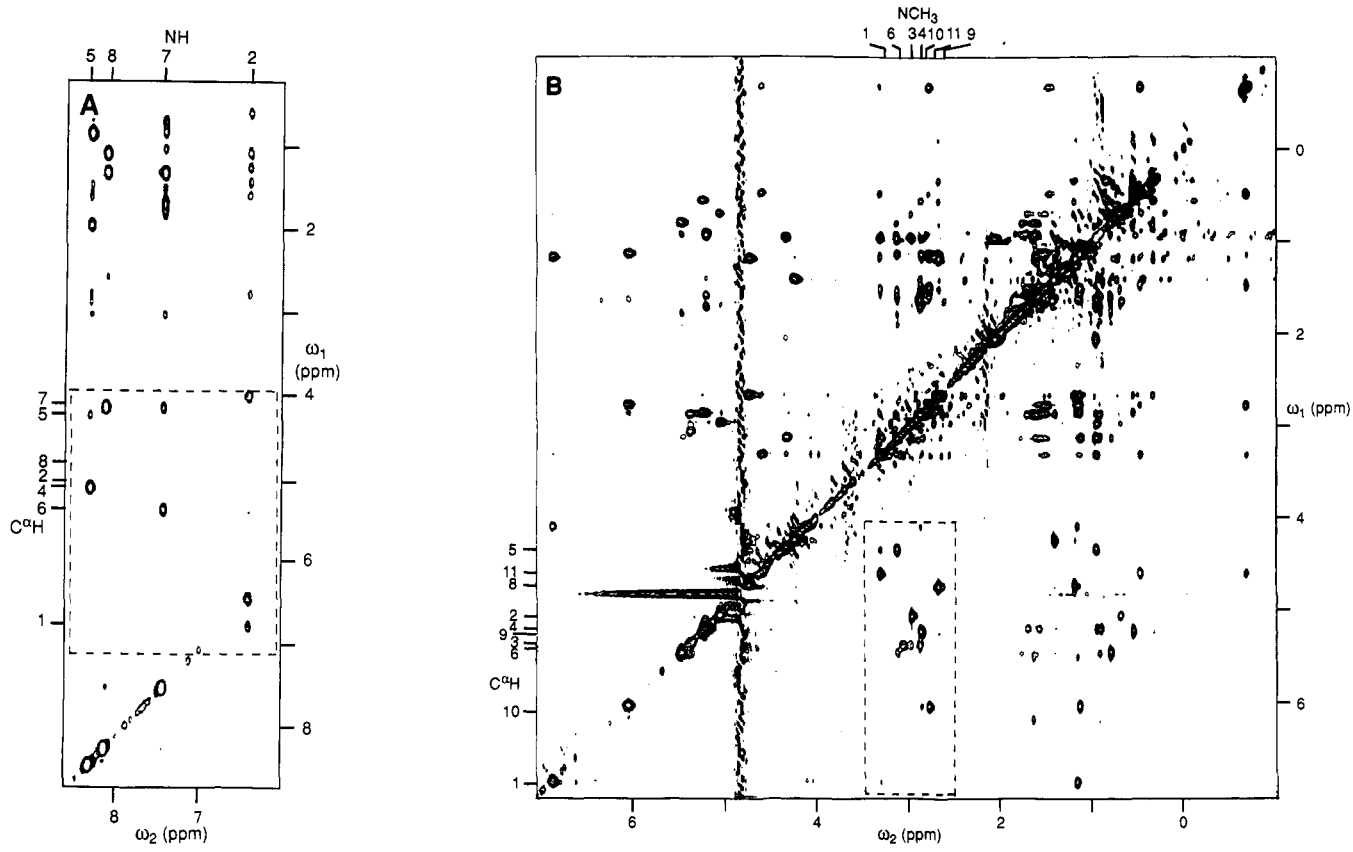


FIGURE 2: [$^1$H,$^1$H]-NOESY spectra of CsA bound to CYP recorded with heteronuclear filters. (A) NOESY spectrum with a $^{15}N(\omega_2)$ half-filter recorded with uniformly $^{15}$N-enriched CsA bound to unlabeled CYP. The region ($\omega_1$ = 0.2–8.6 ppm, $\omega_2$ = 6.0–8.6 ppm) that contains all the cross peaks of the $^{15}N(\omega_2)$-selected subspectrum is shown (0.8 mM complex in 500 $\mu$L of a mixed solvent of 90% $H_2O$/10% $^2H_2O$, 10 mM potassium deuteroacetate, 10 mM potassium phosphate, 0.04% sodium azide, pH 6.0, 25 °C, 85 h measuring time, $^1$H frequency 500 MHz, mixing time $\tau_m$ = 120 ms). The box drawn with broken lines contains all the $C^\alpha H$–NH cross peaks; this spectral region is reproduced in Figure 3. (B) NOESY spectrum with a $^{13}C(\omega_1,\omega_2)$-double-half-filter recorded with uniformly $^{13}$C-enriched CsA bound to unlabeled CYP. The $^{13}C(\omega_1)$-doubly-selected subspectrum is shown (0.8 mM complex in 550 $\mu$L of $^2H_2O$, 10 mM potassium deuteroacetate, 10 mM potassium phosphate, p$^2$H 6.0, 25 °C, $^1$H frequency 500 MHz, mixing time $\tau_m$ = 80 ms). This spectrum resulted from coaddition of three independent experiments recorded in immediate succession with a measuring time of 82 h each. The region shown contains all the peaks that have been identified. The box drawn with broken lines contains all the $C^\alpha H$–$NCH_3$ cross peaks and is reproduced in Figure 3. The chemical shift positions of the $C^\alpha$ protons, the amide protons, and the N-methyl groups are indicated on the left and at the top of the spectra.

NOE cross peaks with the $^{15}$N-bound CsA amide protons are observed (Figure 2A). For the complex with $^{13}$C-labeled CsA, a $^{13}C(\omega_1,\omega_2)$-double-half-filter was used to obtain the doubly selected subspectrum of Figure 2B. This subspectrum contains all the intramolecular NOE's between the $^{13}$C-bound protons of CsA. Double half-filters were described in detail elsewhere (Otting & Wüthrich, 1989, 1990), and the complete set of four subspectra obtained with the [$^{13}$C]CsA–CYP complex was recently presented (Wider et al., 1990).

In homonuclear 2D $^1$H NMR spectra recorded with a $^{15}N(\omega_2)$ half-filter or a $^{13}C(\omega_1,\omega_2)$-double-half-filter, the number of resonances for amide, $C^\alpha$, and N-methyl protons expected for CsA could be identified and distinguished from the side-chain resonances (in the NOESY spectra of Figure 2, the spectral regions containing cross peaks between these protons are identified with broken lines). In a first step, the following spin systems were recognized in $^{13}C(\omega_1,\omega_2)$-doubly-selected COSY or TOCSY experiments with complexes containing fully $^{13}$C-labeled CsA: The $C^\alpha H$–$C^\beta H_3$ fragments of the two alanines; the cross peak between the geminal $C^\alpha$ protons of Sar; complete side-chain spin systems for Abu, the two valines, and one leucine; an $AMX_3$ fragment; two isopropyl groups; and a presumed $C^\alpha H$–$C^\beta H$–$C^{\beta\prime} H$ fragment. The amide protons were connected to their respective side-chain spin systems by TOCSY-relayed [$^{15}$N,$^1$H]-COSY, which provided a distinction between the Val 5 and MeVal 11 spin systems.

In a second step, we established the cyclic sequential assignment pathway via $d_{\alpha N}$ and $d_{\alpha NQ}$ NOE connectivities. The sequential order of free and methylated amide groups (Figure 1) and the cyclic nature of the resulting assignment path (Figure 3) provided important internal checks on the result obtained, which further had to yield the correct placement for the seven side-chain spin systems that had already been identified; the only identified Leu spin system was found to belong to MeLeu 4. Since the N-methyl groups had to be connected to their corresponding side chains by NOE connectivities, it was crucial to have these multiple checks on the sequential assignment. The sequential assignments obtained with $d_{\alpha N}$ and $d_{\alpha NQ}$ were further confirmed by sequential NOE connectivities $d_{\beta N}$, $d_{\beta NQ}$, $d_{NN}$, $d_{NNQ}$, $d_{NQN}$, and $d_{NQNQ}$ (Figure 4).

In a third step, the side-chain assignments were completed by further analysis of [$^{13}$C,$^1$H]-COSY spectra and NOESY spectra of a complex containing fully $^{13}$C-labeled CsA bound to unlabeled CYP. In [$^{13}$C,$^1$H]-COSY two protons that were known from the sequential assignments to belong to MeBmt 1 could be assigned as $C^\alpha H$ and $C^\beta H$ from the characteristic $^{13}$C chemical shift of 58.8 ppm for $C^\alpha$ and 74.7 ppm for $C^\beta$, and the same holds for the two allyl proton–carbon correlation peaks of MeBmt 1. In the [$^{13}$C,$^1$H]-COSY spectrum of biosynthetically directed fractionally $^{13}$C-labeled CsA (Senn et al., 1989; Neri et al., 1989) bound to unlabeled CYP, the

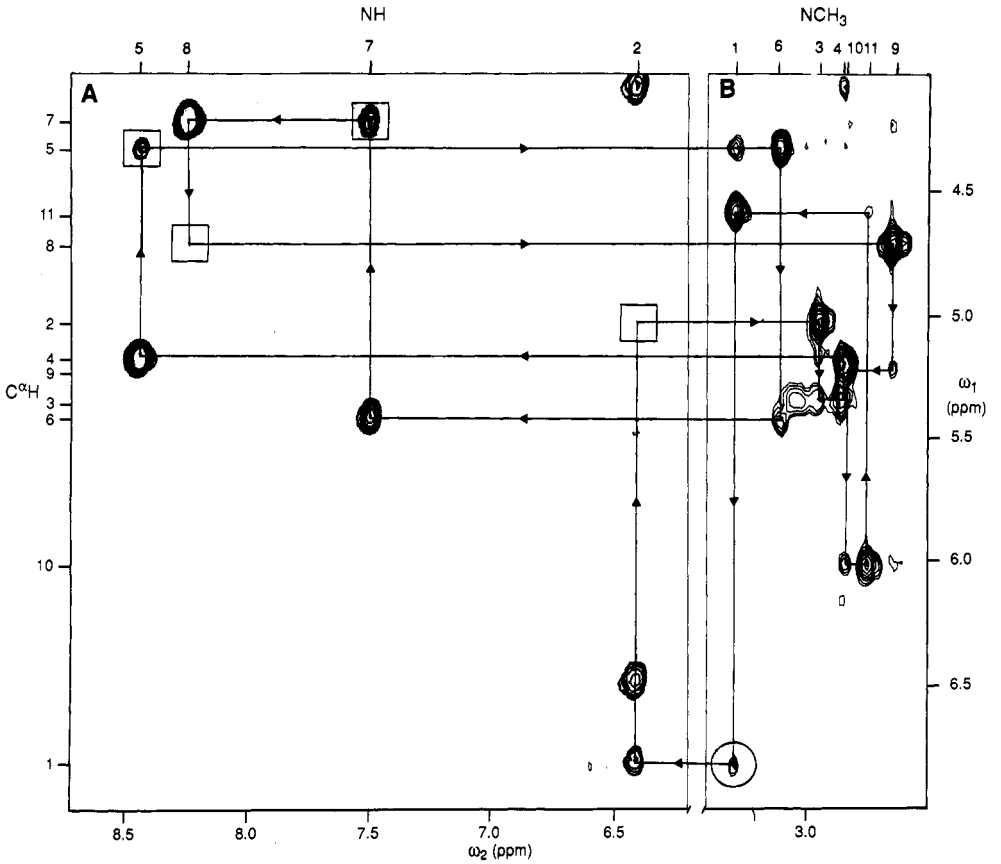


FIGURE 3: Illustration of the sequential assignment procedure via $d_{\alpha N}$ and $d_{\alpha NQ}$ connectivities in CsA bound to CYP. The following parts of the spectra in Figure 2 are used: (A) The region containing cross peaks between amide protons and $C^{\alpha}$ protons in the $^{15}N(\omega_2)$-selected NOESY subspectrum of Figure 2A. (B) The region containing cross peaks between $NCH_3$ and $C^{\alpha}$ protons in the $^{13}C$ $(\omega_1,\omega_2)$-doubly-selected NOESY subspectrum of Figure 2B. The cyclic assignment pathway is indicated with straight lines and arrows, leading from the circled intraresidual $NCH_3$–$C^{\alpha}H$ cross peak of MeBmt 1 clockwise around the structure of Figure 1 and back to the point of departure. The chemical shifts of the individual amide protons and N-methyl groups are indicated at the top and identified by the sequence positions (Figure 1). On the left, the same information is given for the $C^{\alpha}$ protons. The locations of the four intraresidual amide proton–$C^{\alpha}$ proton COSY cross peaks in the spectrum A are indicated with square frames, which contain in two instances the corresponding intraresidual amide proton–$C^{\alpha}H$ NOE cross peak.

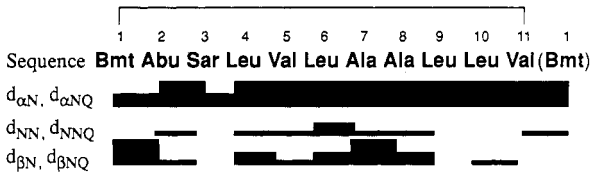


FIGURE 4: Survey of the sequential assignments of CsA bound to CYP. Below the amino acid sequence, thin, medium, and thick bars indicate sequential NOE connectivities represented by weak, medium, and strong NOESY cross peaks, respectively. Note that four different combinations of sequential NOE's between NH and $NCH_3$ may be present in CsA (Figure 1).

four remaining unassigned methyl groups were distinguished by their carbon–carbon coupling patterns along $\omega_1$ (Figure 6): $C^{\eta}H_3$ of MeBmt 1 has a distinctly larger one-bond carbon–carbon coupling ($^1J_{CC} \approx 42$ Hz) than all other methyl groups because it is bound to an allylic carbon, and $C^{\delta}H_3$ of MeBmt 1 is a singlet because it is incorporated into CsA as a one-carbon fragment (Kobel & Traber, 1982). The $C^{\beta}H$ chemical shift of MeBmt 1 obtained from the sequential assignments was found to coincide with the A spin of the $AMX_3$ fragment found in COSY, which was thus assigned as $C^{\beta}H$–$C^{\gamma}H$–$C^{\delta}H_3$ in MeBmt. In the $^{13}C(\omega_1,\omega_2)$-doubly-selected NOESY spectrum of a complex containing fully $^{13}C$-labeled CsA (Figure 2B), there were two NOE's from a resonance line at 2.31 ppm to both $C^{\gamma}H$ and $C^{\delta}H_3$ of MeBmt. This line was therefore assigned to one or both of the $\delta$-protons of MeBmt 1. Of the

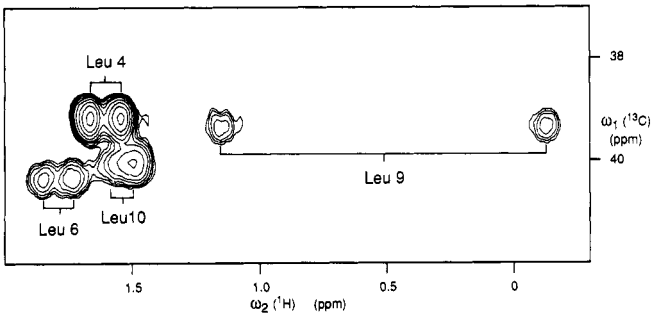


FIGURE 5: Identification of the leucine $\beta$-methylene groups in CsA bound to CYP in a [$^{13}C$,$^1H$]-COSY spectrum of fully $^{13}C$-labeled CsA bound to unlabeled CYP. The resonance positions of the individual $\beta$-protons and $\beta$-carbons in MeLeu 4, MeLeu 6, MeLeu 9, and MeLeu 10 are indicated in the figure (0.8 mM CsA–CYP complex in 550 $\mu$L of $^2H_2O$, 10 mM potassium deuteroacetate, 10 mM potassium phosphate, p$^2$H 6.0, 25 °C, $^1H$ frequency 500 MHz).

two allyl proton lines, the one at 6.18 ppm displayed a NOE to the $\eta$-methyl resonance of MeBmt 1 at 1.62 ppm and was therefore assigned to the $\zeta$-proton. The $C^{\beta}$-H correlation peaks of the four MeLeu residues were well separated in a distinct spectral region of the [$^{13}C$,$^1H$]-COSY spectrum and could be assigned from their unique chemical shifts (Figure 5) (Wüthrich, 1976, 1986). MeLeu 6 was found to contain the $C^{\alpha}H$–$C^{\beta}H$–$C^{\beta'}H$ fragment and one of the two isopropyl groups that were previously identified with COSY and TOCSY. The two fragments were combined on the basis of NOE's from

Table I: $^1$H Chemical Shifts, $\delta$ (ppm), for CsA Bound to CYP at pH 6.0 and 25 °C

| residue | chemical shift, $\delta$ (ppm)[a] | | | |
|---|---|---|---|---|
| | NH/NCH$_3$ | $\alpha$H | $\beta$H | others |
| Me$\beta$mt 1 | 3.28 | 6.82 | 4.05 | $\gamma$H 1.49; $\delta$CH$_2$ 2.31; $\delta$CH$_3$ 1.14; $\epsilon$H 5.54; $\zeta$H 6.18; $\eta$CH$_3$ 1.62 |
| Abu 2 | 6.42 | 5.01 | 1.67, 1.56 | $\gamma$CH$_3$ 0.68 |
| Sar 3 | 2.93 | 3.02, 5.32[b] | | |
| MeLeu 4 | 2.84 | 5.15 | 1.68, 1.56 | $\gamma$H 1.38; $\delta^1$CH$_3$ *0.93*; $\delta^2$CH$_3$ 0.88 |
| Val 5 | 8.44 | 4.30 | 2.02 | $\gamma^1$CH$_3$ *0.95*; $\gamma^2$CH$_3$ *0.94* |
| MeLeu 6 | 3.10 | 5.42 | *1.85*, *1.74* | $\gamma$H 1.58; $\delta^1$CH$_3$ *0.90*; $\delta^2$CH$_3$ *0.78* |
| Ala 7 | 7.49 | 4.20 | 1.38 | |
| D-Ala 8 | 8.24 | 4.69 | 1.16 | |
| MeLeu 9 | 2.63 | 5.19 | 0.88, −0.12 | $\gamma$H 0.79; $\delta^1$CH$_3$ *0.32*; $\delta^2$CH$_3$ *0.54* |
| MeLeu 10 | 2.83 | 5.99 | 1.60, 1.57 | $\gamma$H 1.48; $\delta^1$CH$_3$ *1.11*; $\delta^2$CH$_2$ *1.12* |
| MeVal 11 | 2.74 | 4.56 | 1.43 | $\gamma^1$CH$_3$ *0.46*; $\gamma^2$CH$_3$ *−0.69* |

[a] Measured relative to internal TSP [3-(trimethylsilyl)propanesulfonic acid]. For methylene groups two chemical shifts are given only when two resolved signals were observed. Stereospecific assignments are indicated in italics. For the isopropyl methyl groups of Val and Leu these were obtained by biosynthetically directed fractional $^{13}$C labeling, and for C$^\beta$H$_2$ of MeLeu 6 they were obtained by HABAS (H$^{\beta 2}$ is listed first). Chemical shifts which are more than 0.2 ppm different relative to CsA in chloroform solution (Kessler et al., 1985) are indicated as follows: underlined, shifted to higher field; overlined, shifted to lower field. [b] Probable individual assignments of the C$^\alpha$ protons of Sar 3 were obtained by analysis of structures calculated with either assignment of the two relevant NOE's (Table SI): The sequential NOE from C$^{\alpha 2}$H of Sar 3 to NCH$_3$ of MeLeu 4 could only be satisfied with an assignment to C$^{\alpha 2}$H. C$^{\alpha 1}$H is then coplanar with the carbonyl group of Sar 3, which could explain its high-field shift. Structure calculations using this individual assignment in the place of the pseudoatom did not noticeably improve the final structures, and it was therefore not included in the final input data set.

C$^\alpha$H to C$^\delta$H$_3$ and C$^{\delta'}$H$_3$ and from NCH$_3$ to the two methyl groups. MeLeu 9 was found on the basis of NOE's from C$^\alpha$H to C$^\beta$H, C$^{\beta'}$H, C$^\gamma$H, C$^\delta$H$_3$, and C$^{\delta'}$H$_3$ and from NCH$_3$ to C$^{\beta'}$H, C$^\gamma$H, C$^\delta$H$_3$, and C$^{\delta'}$H$_3$ to contain the other isopropyl group identified by COSY. The MeLeu 10 side-chain spin system was assigned from NOE's between C$^\alpha$H and the side-chain protons, by using the two yet unassigned methyl resonances. In summary, all $^1$H resonances of CsA bound to CYP could be assigned, with the possible exception of C$^{\delta'}$H of MeBmt 1.

Stereospecific assignments for all six pairs of diastereotopic isopropyl methyls were obtained by the method of biosynthetically directed fractional $^{13}$C labeling (Senn et al., 1989), Neri et al., 1989). Although in two of the six isopropyl groups the methyl resonances had nearly degenerate $^1$H chemical shifts, and additional methyl proton lines were strongly overlapped near 0.93 ppm, all the methyl resonances were well separated in the $^{13}$C dimension (Figure 6). The assigment of the *pro-R* methyl groups, $\gamma^1$ and $\delta^1$, respectively, was straightforward since they were represented by well-resolved doublets in the $^{13}$C dimension (Neri et al., 1989). For each *pro-S* methyl group, we observed a singlet superimposed by a much weaker isotope-shifted doublet, which coalesced into a cross peak with barely resolved fine structure.

The $^1$H chemical shifts of CsA bound to CYP are compiled in Table I. Also indicated are those protons with shifts of more than 0.2 ppm relative to CsA in chloroform solution (Kessler et al., 1985). Large chemical shift differences were found for the backbone and C$^\beta$ protons of nearly all residues, but only for the side-chain protons of MeBmt 1, MeLeu 9, and MeVal 11.

*Preparation of the Input for Structure Calculations.* The general strategy described in Table 10.1 of Wüthrich (1986) was followed to relate NOE intensities with upper distance bounds. Since NOE distance constraints were collected from NOESY spectra recorded with different heteronuclear filters, special care was taken to rely on *empirical calibration* of the relations between NOE intensities and corresponding $^1$H–$^1$H *distance constraints. To obtain additional reference points,* the dihedral angle dependence was calculated for the distances $d_{NQ\alpha}(i,i)$ and $d_{\alpha NQ}(i,i+1)$, where Q stands for a pseudoatom located centrally with respect to the three protons of the

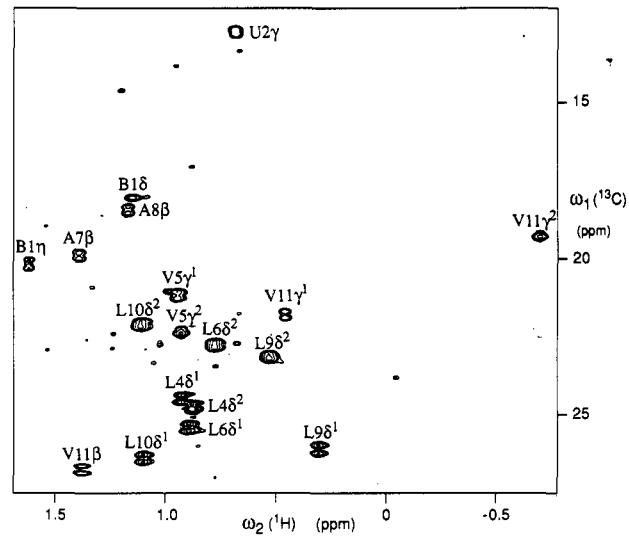


FIGURE 6: Individual assignments of the isopropyl methyl groups of valine and leucine in CsA bound to CYP. The region containing all the CsA methyl resonances is shown for a [$^{13}$C,$^1$H]-COSY spectrum recorded with a complex of biosynthetically directed fractionally $^{13}$C-labeled CsA bound to unlabeled CYP. The cross peaks are labeled with the one-letter symbol of the amino acid symbols: B, (4*R*)-4-[(*E*)-2-butenyl]-4,*N*-dimethyl-L-threonine; U, $\alpha$-aminobutyric acid; V stands for valine and N-methylvaline, A for L- and D-alanine, and L for *N*-methylleucine; a greek letter indicates the carbon atom position and a superscript the branch number of the carbon atom (0.8 mM complex in 550 $\mu$L of $^2$H$_2$O, 10 mM potassium deuteroacetate, 10 mM potassium phosphate, p$^2$H 6.0, 25 °C, $^1$H frequency 500 MHz, 20 Hz digital resolution recorded in $t_1$, zero filled to a 6 Hz final digital resolution in $\omega_1$).

N-methyl group [for the notation used, see p 117 in Wüthrich (1986)]. Standard ECEPP geometry was used for the amino acid residues [for details of the calculation, see Billeter et al. (1982)]. Figure 7 shows that for $d_{NQ\alpha}(i,i)$ both the lower and upper limits are significantly longer than for $d_{N\alpha}$ (Wüthrich, 1986), whereas for $d_{\alpha NQ}(i,i+1)$ the lower limit is nearly the same as for $d_{\alpha N}(i,i+1)$ (Billeter et al., 1982) and only the upper limit is approximately 0.5 Å longer.

Details of the analysis of the $^1$H–$^1$H NOEs are given in the supplementary materials, which also include Table SI with a complete list of all NOE upper distance constraints. Figure

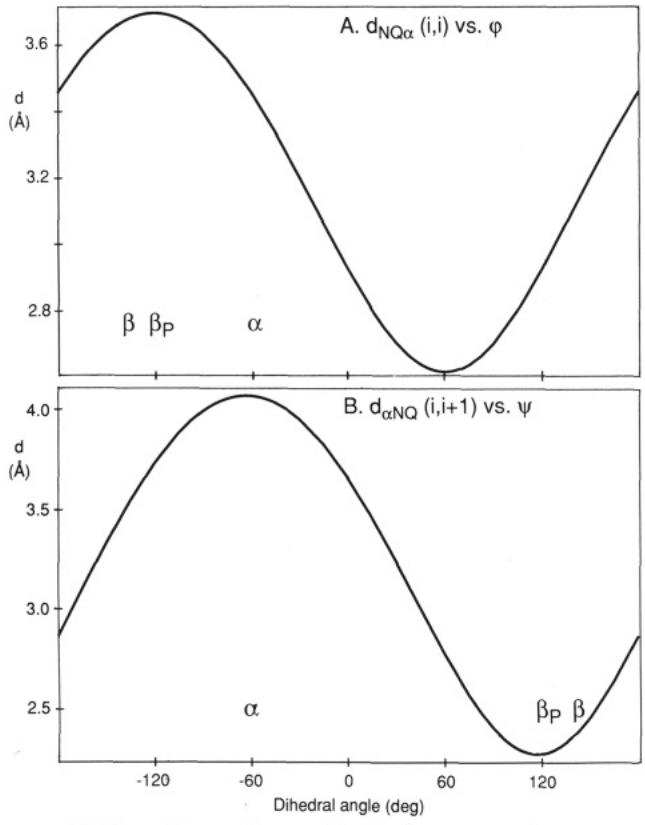


FIGURE 7: Dependence of intraresidual and sequential distances on the intervening dihedral angle in N-methylated polypeptides. (A) Intraresidual distance between the pseudoatom NQ in the center of the three N-methyl protons and the $C^{\alpha}$ proton, $d_{NQ\alpha}(i,i)$, versus $\phi_i$. (B) Sequential distance $d_{\alpha NQ}(i,i+1)$ versus $\psi_i$. The values of $\phi$ and $\psi$ that correspond to a regular $\alpha$-helix or a parallel or antiparallel $\beta$-sheet are indicated by the letters $\alpha$, $\beta$p, and $\beta$, respectively.

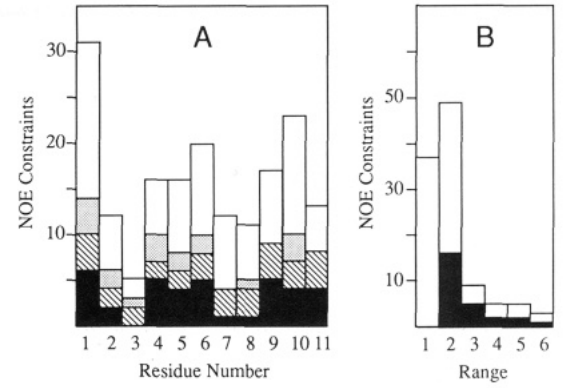


FIGURE 8: (A) Plot of the number of NOE distance constraints per residue versus the amino acid sequence of CsA bound to CYP. All interresidual constraints appear twice, once for each of the two interacting residues. Four types of NOE constraints are specified as follows (Wüthrich, 1986): black, intraresidual; hatched, sequential backbone; dotted, medium- and long-range backbone; white, interresidual with side chain protons. (B) Plot of the number of NOE distance constraints versus their range along the amino acid sequence of CsA bound to CYP. Two types of NOE constraints are specified as follows: black, backbone–backbone constraints; white, backbone–side chain or side chain–side chain constraints. Because of the cyclic structure of CsA, the range cannot exceed 6.

8 shows plots of the number of NOE constraints per residue vs the sequence and of the number of NOE's vs their range along the sequence. Note that because of the cyclic structure, the maximum range is 6.

Supplementary constraints were obtained from the $^3J_{HN\alpha}$ coupling constants measured with a 1D version of *J*-modulated [$^{15}$N,$^1$H]-COSY (Neri et al., 1990). The resulting allowed ranges of $^3J_{HN\alpha}$ were Abu 2, >8 Hz; Val 5, 4.1–5.8 Hz; Ala 7, 4.0–5.9 Hz; D-Ala 8, 5.1–6.5 Hz. The combined analysis of NOE's and spin–spin coupling constants by the program HABAS (Güntert et al., 1989) yielded additional dihedral angle constaints for MeLeu 6 of $\psi = 170°$ to $-140°$ and $\chi^1 = -60°$ to $-10°$ and a constraint for Val 5 of $\chi^1 = 40°$ to $-40°$.

With regard to the distance geometry calculations, the following qualitative observations made during the resonance assignments and the collection of distance constraints are of importance: All sequential NOE's $d_{\alpha N}$ or $d_{\alpha NQ}$ were strong or medium-strong (Figures 3 and 4), and no sequential NOE's between $C^{\alpha}$ protons were detected (Figure 2B). Furthermore, to assess whether twisted amide bonds would be compatible with the observed NOE's, the sequential distance $d_{\alpha NQ}$ (Figure 7) was calculated as a function of both intervening angles $\psi$ and $\omega$. It was found that $d_{\alpha NQ}$ distances shorter than 3.0 Å are only compatible with $\omega$ angles from 130° to −130°. From this it was concluded that there are no cis amide bonds in CsA bound to CYP, and the structure was calculated assuming that $\omega = 180°$ for all peptide bonds.

*Calculation of the CsA Structure from the NMR Data.* For the distance geometry calculations with the program DISMAN, the input consisted of the NMR constraints discussed in the preceding section and a set of constraints enforcing the cyclic structure as described under Materials and Methods. The influence of the artificial cyclization on the resulting structures was assessed by comparison of calculations starting from randomly chosen starting conformations of the linear chain with MeBmt 1 at the N-terminus and MeVal 11 at the C-terminus or with Ala 7 and MeLeu 6 as the terminal residues. It was found that the location chosen for the ends of the linear chain and the use of the extrinsic cyclization constraints had at most a minimal effect on the calculated structures. We therefore arbitrarily decided to place the cyclization between residues 6 and 7.

For the final structure calculation, 3500 randomly chosen starting conformations of the open chain of CsA with Ala 7 at the N-terminus and MeLeu 6 at the C-terminus were used. The DISMAN calculations were taken through all 11 target levels. At levels one and two, 200 optimization cycles were calculated, at levels three to ten, 100 cycles, and at level 11, 500 cycles to achieve convergence. The relative weight of NOE constraints, van der Waals constraints, and dihedral angle constraints was 1, 0.2, and 10, respectively. At the completion of the calculation at level 11 the van der Waals weighting was increased to 0.5 and another 300 optimization cycles were added. Final structures with a target function value smaller than 1.5 Å$^2$ were retained. The 181 structures selected by using this criterion were subjected to restrained energy minimization with the program FANTOM (Schaumann et al., 1990), using the same constraint set as was used for the distance geometry. From among the energy-refined structures, 123 species were selected with the following criteria: maximum violation of upper distance limits ≤0.5 Å, of angle constraints ≤5.0°, and of cyclization constraints ≤0.1 Å; $\omega = 180° \pm 20°$ for the peptide bond enforced by the cyclization; the sum of violations of upper distance limits, the sum of violations of angle constraints, the total physical energy, and the total nonbonding energy all had to be equal to or smaller than the sum of the mean and the standard deviation of the corresponding quantity. Three pairs of structures among these 123 species had identical torsion angles to within 1°. There were therefore only 120 independent solutions to the minimization problem, which are all good solutions with respect to residual violations of the input data (Table II). Since CsA is very

Table II: Analysis of the 120 Energy-Minimized Structures Used To Represent the Solution Conformation of CsA Bound to CYP

| quantity | average value ± standard deviation (range) |
|---|---|
| conformational energy[a] | |
| total (kcal/mol) | 126.0 ± 14.1 (99.6–158.7) |
| electrostatic (kcal/mol) | 65.9 ± 1.1 (62.7–68.3) |
| H-bond (kcal/mol) | −1.5 ± 1.2 (−3.8 to −0.3) |
| torsional (kcal/mol) | 19.1 ± 3.5 (12.6–27.8) |
| Lennard-Jones (kcal/mol) | 42.6 ± 12.4 (20.9–71.9) |
| residual NOE distance constraint violations[b] | |
| number >0.2 Å | 5.32 ± 1.48 (2–11) |
| sum (Å) | 2.64 ± 0.49 (1.53–3.69) |
| maximum (Å) | 0.39 ± 0.05 (0.25–0.47) |
| residual dihedral angle constraint violations[b] | |
| number >0° | 3.22 ± 0.93 (1–6) |
| sum (deg) | 0.83 ± 0.44 (0.10–1.96) |
| maximum (deg) | 0.49 ± 0.28 (0.09–1.39) |
| residual cyclization constraint violations[b] | |
| number >0.1 Å | 0.0 ± 0.0 (0–0) |
| sum (Å) | 0.14 ± 0.02 (0.10–0.18) |
| maximum (Å) | 0.02 ± 0.00 (0.02–0.03) |
| peptide angle (deg) | 176.4 ± 6.1 (160.2–189.5) |
| average of the global pairwise RMSDs (Å) | |
| backbone atoms N, $C^{\alpha}$, C′ | 0.58 ± 0.19 (0.00–1.24) |
| all heavy atoms | 1.19 ± 0.25 (0.01–2.00) |
| average of the local RMSDs for all tripeptide segments (Å) | |
| backbone atoms N, $C^{\alpha}$, C′ | 0.21 ± 0.04 (0.13–0.28) |

[a] The balance between the conformational energy and the restraint energy is determined by the following selection of the parameters in eq 4 in Schaumann et al. (1990): the exponent was set to $n = 4$, and the distance violation that corresponds to $kT/2$ ($T = 298$ K) was set to 0.2 Å for NOE upper distance limits and 0.03 Å for the cyclization constraints. In the potential accounting for the dihedral angle restraints (Braun, 1987), a violation of 1° corresponds to an energy of $100kT/2$. [b] The input data set consisted of 108 NOE distance constraints, 22 dihedral angle constraints, and 9 cyclization constraints.

Table III: Backbone Dihedral Angles in the Solution Conformation of CsA Bound to CYP

| amino acid | dihedral angle ± standard deviation (deg)[a] $\phi$ | $\psi$ | $\omega$ |
|---|---|---|---|
| MeBmt 1 | −125 ± 14 | −167 ± 15 | −176 ± 3 |
| Abu 2 | −131 ± 13 | 99 ± 29 | 180 ± 4 |
| Sar 3 | 138 ± 24 | −41 ± 14 | −179 ± 4 |
| MeLeu 4 | −150 ± 22 | 92 ± 17 | 180 ± 2 |
| Val 5 | −75 ± 3 | 136 ± 7 | 177 ± 2 |
| MeLeu 6 | −114 ± 6 | −159 ± 14 | 176 ± 6 |
| Ala 7 | −80 ± 1 | 172 ± 9 | 178 ± 1 |
| D-Ala 8 | 83 ± 4 | −156 ± 6 | −177 ± 4 |
| MeLeu 9 | −126 ± 7 | 86 ± 5 | 180 ± 2 |
| MeLeu 10 | −117 ± 17 | 153 ± 18 | 180 ± 3 |
| MeVal 11 | −131 ± 11 | 80 ± 15 | 177 ± 5 |

[a] The numbers are the mean values and standard deviations of the dihedral angles in the 120 energy-minimized structures used to represent the solution conformation of CsA bound to CYP.

hydrophobic but does not form a buried core, there are no sizeable negative energy terms. The total conformational energy is therefore positive (Table II), which is in contrast with typical globular proteins. The 120 conformers represent a well-defined conformation of the polypeptide backbone, as can be seen from the small global and local RMSD values for the backbone atoms (Table II) and in the drawings of Figure 9A. The mean values of the dihedral angles and their standard deviations, which define the solution conformation of the polypeptide backbone of CsA bound to CYP, are listed in Table III.

As a final qualitative check of the compatibility of the structures obtained with the experimental input, we searched the structures for short distances, i.e., <4.0 ± 1.5 Å, that would not have been observed as NOE's. We found no evidence that such short $^1H$–$^1H$ distances would have escaped detection.

## Discussion

*The Solution Conformation of CsA Bound to CYP.* The structure of bound CsA contains no regular secondary structure and no intramolecular hydrogen bonds. The two antiparallel backbone segments from residues 4 to 7 and 9 to 2 have their planar peptide bonds rotated out of the plane defined by the cyclic polypeptide backbone, which contrasts with regular β-strands. In the strand from MeLeu 9 to Abu 2, the residue MeVal 11 bulges out. Five of the seven $NCH_3$ moieties are buried to some degree inside the cyclosporin ring, while the four amide protons are exposed to the outside. This coincides with the observation that the amide proton exchange is fast for Val 5, Ala 7 and D-Ala 8. For Abu 2 the half-life for NH exchange is approximately 3 days at pH 6.0 and 25 °C. As there is no obvious acceptor group in CsA, we attribute the slow exchange to an intermolecular hydrogen bond of the amide proton of Abu 2 with CYP (see below). Of the 11 carbonyl oxygen atoms, all but one are to some extent exposed, the exception being MeLeu 4, for which the C=O group is completely buried.

In the view of Figure 9B, the side chains of MeBmt 1, MeLeu 4, MeLeu 6, and MeLeu 10 are in front of the plane occupied by the polypeptide backbone, and the remaining four bulky side chains of Abu 2, Val 5, MeLeu 9, and MeVal 11 are behind the backbone plane and point away from the reader. Except for Val 5 and MeLeu 6, for which the $\chi^1$ angles are well defined at about 177° and −54°, respectively, the other long side chains were mainly constrained by long-range NOE's with peripheral groups of protons. Although the spatial orientation is thus quite well defined (Figure 9B), the individual dihedral angles $\chi^n$ vary within rather wide ranges. Most prominent is the side chain of MeBmt 1, which is folded back over the molecule and makes contacts with the isopropyl groups of MeLeu 4 and MeLeu 6 across the ring. It is also apparent that the side chains 1, 4, 6, and 10 form a quite compact cluster over the cyclic backbone. In contrast, the side chains 2, 9, and 11 located behind the backbone plane point away from the core of the molecule.

*Comparison of the Structure of CsA Bound to CYP with Free CsA.* Overall the NMR structure of CsA bound to CYP represents a new cyclosporin conformation, which to the best of our knowledge has not been observed so far. It contains features that have been predicted from other data, for example that the side chain of MeBmt 1 is folded back onto the molecule (Quesniaux et al., 1988). When compared to the crystal structure of free CsA, there are important differences and only few similarities. The global RMSD between the backbones of the two structures is 2.5 Å, and numerous NOE distance constraints measured for CsA bound to CYP are sizeably violated in the crystal structure of CsA. In the crystal structure of CsA there is a cis amide bond between residues 9 and 10, whereas in the CsA bound to CYP all amide bonds are trans. The crystal structure of CsA contains three transannular hydrogen bonds and one additional hydrogen bond from NH of D-Ala 8 to C′=O of MeLeu 6, but there are no intramolecular hydrogen bonds in the conformation of CsA bound to CYP. Instead, the latter contains 5 N-methyl groups within the ring formed by the polypeptide backbone. In the crystal structure, all but one of the $NCH_3$ groups are oriented toward the molecular surface, whereas in the bound CsA only two $NCH_3$ groups are exposed, one of which is the $NCH_3$ group of MeVal 11, which is buried in the crystal. In both structures the same groups of bulky side chains are clustered together on the two sides of the backbone plane.

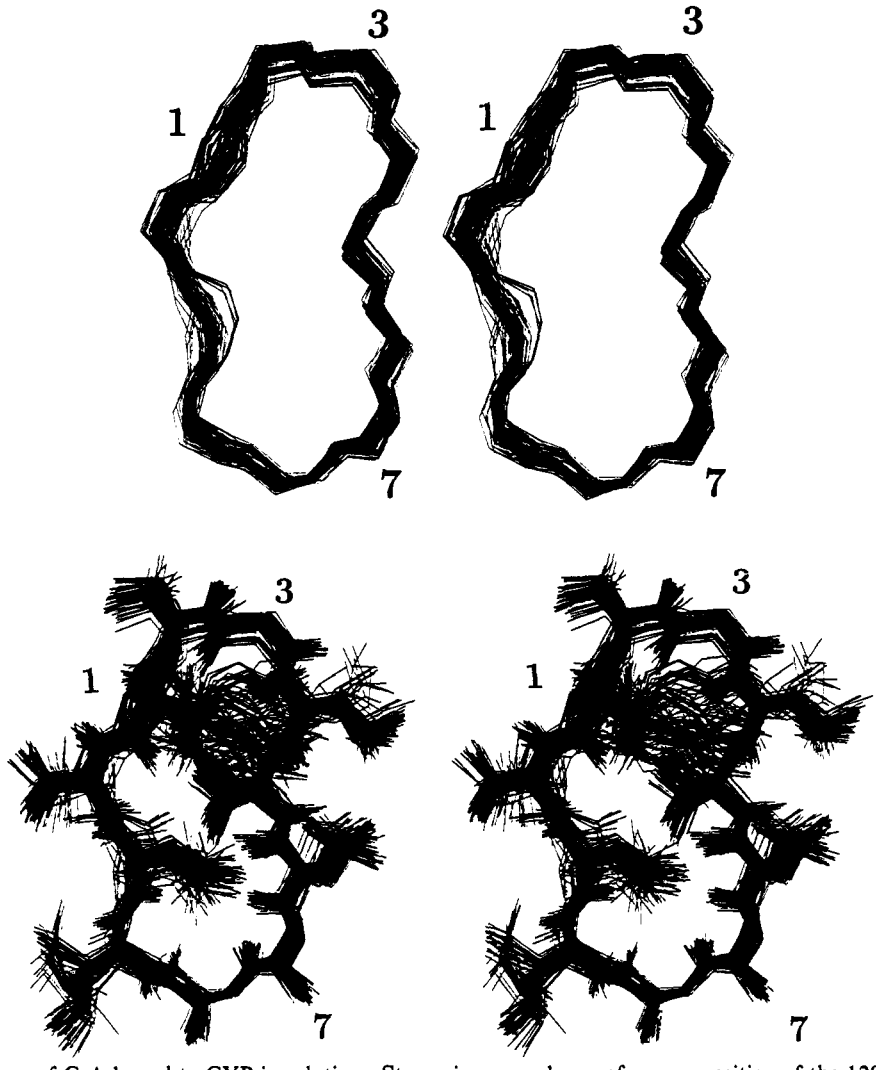


FIGURE 9: NMR structure of CsA bound to CYP in solution. Stereoviews are shown of a superposition of the 120 best energy-minimized structures characterized in Table II. (A) The bonds connecting the backbone atoms N, $C^{\alpha}$, and C′ are drawn. (B) The bonds connecting all heavy atoms are shown, with the same orientation as in A.

However, in the views of Figure 10 the side chains of MeBmt 1, MeLeu 4, MeLeu 6, and MeLeu 10 are located behind the ring in the crystal structure but above the ring in CsA bound to CYP.

A recently reported NMR structure of CsA in chloroform solution (Kessler et al., 1990) is closely similar to the crystal structure. In particular, the four hydrogen bonds identified in the crystal structure are preserved, and the side chain of MeBmt 1 is also folded back onto the molecule (Figure 10). Overall, a detailed comparison between the NMR structures of CsA in chloroform solution and bound to CYP leads to similar conclusions as the comparison of the bound CsA with the crystal structure, i.e., there are important conformational differences of the type detailed in the preceding paragraph.

*Influence of the Intermolecular Contacts between CsA and CYP.* In addition to the collection of intramolecular NOE's in CsA, which is the principal subject of this paper, numerous intermolecular NOE's between protons of CsA and of CYP were observed in the $^{13}C(\omega_1)$-selected $^{13}C(\omega_2)$-filtered and $^{13}C(\omega_1)$-filtered $^{13}C(\omega_2)$-selected subspectra from NOESY recorded with a $^{13}C(\omega_1,\omega_2)$-double-half-filter (Wider et al., 1990). Overall, these data show that there are close contacts of CYP with the residues MeBmt 1, Abu 2, Sar 3, MeLeu 9, MeLeu 10, and MeVal 11 of CsA. This is schematically visualized in Figure 11. From Table I it is seen that many protons of these residues (and none of the other side chains) have large chemical shift differences relative to free CsA. Very probably, because of the intermolecular steric constraints that can be expected to create a similar environment to that experienced by interior residues in globular proteins (Wüthrich, 1986), the side chains of residues 9–3, which interact with CYP, are among the most strongly confined parts of the CsA molecule. Nonetheless, these side chains are relatively poorly defined in the present CsA structure (Figure 9B, Table III). This apparent discrepancy must be due largely or entirely to the fact that in the present structure determination neither intermolecular NOE constraints nor intermolecular steric constraints were included in the input for the structure calculations.

The chemical shift differences between free CsA and CsA bound to CYP can be qualitatively rationalized from the present preliminary information on the intermolecular interactions. Many of the intermolecular NOE's are with aromatic rings of CYP. In particular, Trp 121 in CYP interacts with CsA protons. This explains that the shift differences cannot have a clear trend toward high or low field, because both the sign and the magnitude of the ring current shifts depend on the relative orientation of the aromatic rings and the CsA protons (Wüthrich, 1976). We even found CsA protons involved in strong NOE's with aromatic protons of CYP that were hardly shifted relative to CsA in $CDCl_3$ solution, e.g., the $NCH_3$ group of MeVal 11 (Table I). The intermolecular

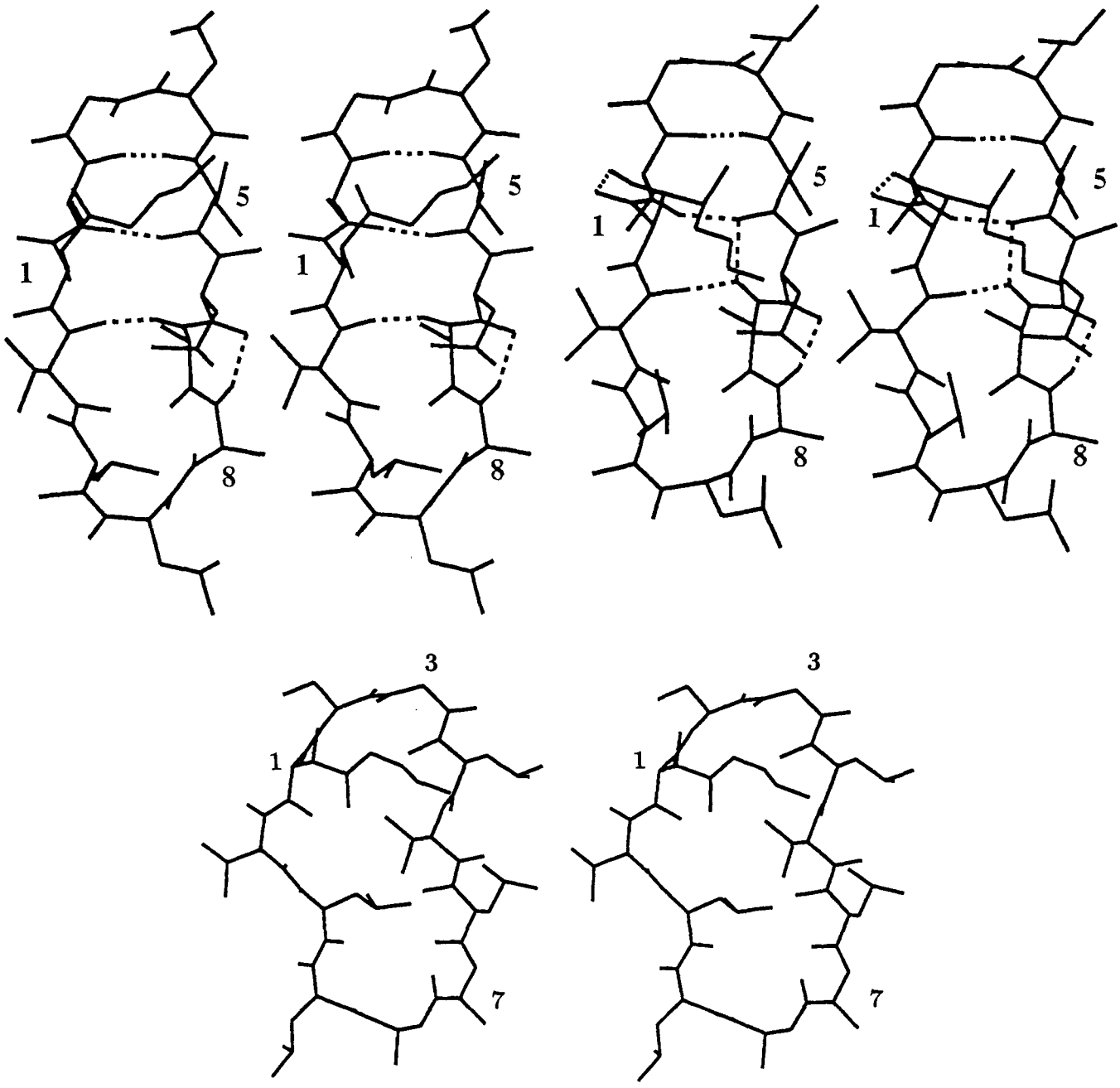


FIGURE 10: Structure of CsA in different environments. Stereoviews are shown of the bonds connecting all heavy atoms. For panels A and B the amide protons of Abu 2, Val 5, Ala 7, and D-Ala 8 are shown, and the hydrogen bonds are indicated by broken lines. (A) X-ray structure of CsA in single crystals (Loosli et al., 1985). (B) NMR structure of CsA in chloroform solution (Kessler et al., 1990). (C) NMR structure of CsA bound to CYP in aqueous solution.

NOE's with aromatic rings of CYP can also explain the observation of an enhancement of the Trp fluorescence upon CsA binding to CYP (Handschumacher et al., 1984). They are further consistent with the hypothesis based on NMR data that the hydrophobic core in CYP contains numerous aromatic rings (Dalgarno et al., 1986), of which many resonance lines shift upon CsA binding (Heald et al., 1990; our unpublished results).

## CONCLUSIONS

All previous discussions on structure–function correlations in CsA were based on the structure of free CsA determined either by X-ray diffraction in single crystals or by NMR in chloroform solution (Loosli et al., 1985; Kessler et al., 1990). Although the present study accounts only partially for the influence of the receptor protein on the conformation of CsA bound to CYP (see the immediately preceeding section), it clearly demonstrates the importance of direct experimental studies with both the free and the receptor-bound effector molecule as a basis for discussions on its structure–function correlations. Most striking is the observation that in the cyclic structure of CsA, which has a greatly reduced accessible conformation space when compared to a corresponding linear polypeptide, the backbone conformation is largely rearranged in the receptor-bound state. As was explained in detail in the immediately preceding section, a more precise description of the spatial arrangement of the amino acid side chains of CsA that are in direct contact with CYP will have to await a detailed characterization of the entire complex, including CYP and its intermolecular interactions. However, already the results presented in this paper, which were obtained without the use of any direct structural information on the receptor

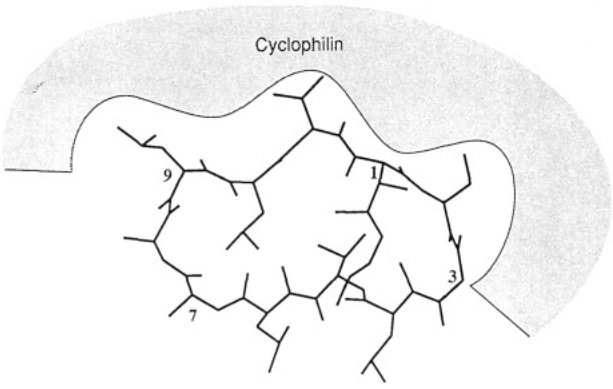


FIGURE 11: Schematic visualization of the intermolecular interactions between CsA and CYP. The best structure of bound CsA from Figure 9 has been docked into a schematic binding site of CYP in such a way that there are contacts with all amino acid residues of CsA for which strong intermolecular NOE's were observed. In the third dimension perpendicular to the planar drawing, the binding site of CYP would have a similar surface and extent as the one depicted here in two dimensions.

protein, should be of interest to those engaged in the design of cyclosporin-related drugs with improved and/or altered activity profiles.

## Acknowledgments

The use of the Cray-XMP/28 of the ETH Zürich is gratefully acknowledged. We thank Prof. H. Kessler for the atom coordinates of the recently published NMR structure of CsA in chloroform solution, and Mr. R. Marani for the careful processing of the manuscript.

## Supplementary Material Available

Table SI showing the NOE distance constraints used as input for the calculation of the structure of cyclosporin A bound to cyclophilin (6 pages). Ordering information is given on any current masthead page.

## References

Billeter, M., Braun, W., & Wüthrich, K. (1982) *J. Mol. Biol. 155*, 321–346.

Billeter, M., Engeli, M., & Wüthrich, K. (1985) *J. Mol. Graphics 3*, 79–83; 97–98.

Bodenhausen, G., & Ruben, D. (1980) *Chem. Phys. Lett. 69*, 185–188.

Borel, J. F., Ed. (1986) *Ciclosporin*, Karger, Basel.

Braun, W. (1987) *Q. Rev. Biophys. 19*, 115–157.

Braun, W., & Go, N. (1985) *J. Mol. Biol. 186*, 611–626.

Dalgarno, D. C., Harding, M. W., Lazarides, A., Handschumacher, R. E., & Armitage, I. M. (1986) *Biochemistry 25*, 6778–6784.

Denk, W., Baumann, R., & Wagner, G. (1986) *J. Magn. Reson. 67*, 386–390.

Eccles, C., Billeter, M., Güntert, P., & Wüthrich, K. (1989) *Abstracts 10th Meeting of the International Society of Magnetic Resonance*, Morzine, France, July 16–21, 1989, p S50.

Elliot, J. F., Lin, Y., Mizel, S. B., Bleakley, R. C., Harnish, D. G., & Paetkau, V. (1984) *Science 226*, 1439–1441.

Emmel, E. A., Verweij, C. L., Durand, D. B., Higgins, K. M., Lacy, E. & Crabtree, G. R. (1989) *Science 246*, 1617–1620.

Fesik, S. W. (1988) *Nature 332*, 865–866.

Fesik, S. W., Luly, J. R., Erickson, J. W., & Abad-Zapatero, C. (1988) *Biochemistry 27*, 8297–8301.

Fesik, S. W., Gampe, R. T., Jr., Eaton, H. L., Gemmacker, G., Olejniczak, E. T., Neri, P., Holzman, T. F., Egan, D. A., Edalji, R., Simmer, R., Helfrich, R., Hochlowski, J., & Jackson, M. (1991) *Biochemistry*, following paper in this issue.

Fischer, G., Wittmann-Liebold, B., Lang, K., Kiefhaber, T., & Schmid, F. X. (1989) *Nature 337*, 476–478.

Griffey, R. H., & Redfield, A. G. (1987) *Q. Rev. Biophys. 19*, 51–82.

Güntert, P., Braun, W., Billeter, M., & Wüthrich, K. (1989) *J. Am. Chem. Soc. 111*, 3997–4004.

Güntert, P., Qian, Y. Q., Otting, G., Müller, M., Gehring, W., & Wüthrich, K. (1991) *J. Mol. Biol. 217*, 531–540.

Haendler, B., Hofer-Warbinek, R., & Hofer, E. (1987) *EMBO J. 6*, 947–950.

Handschumacher, R. E., Harding, M. W., Rice, J., & Drugge, R. J. (1984) *Science 226*, 544–547.

Harrison, R. K., & Stein, R. L. (1990) *Biochemistry 29*, 1684–1689.

Heald, S. L., Harding, M. W., Handschumacher, R. E., & Armitage, I. M. (1990) *Biochemistry 29*, 4466–4478.

Kahan, B. D., Ed. (1988) *Cyclosporine—Nature of the Agent and its Immunologic Actions*, Grune & Stratton, New York.

Kawamukai, M., Matsuda, H., Fuji, W., Utsumi, R., & Komano, T. (1989) *J. Bacteriol. 171*, 4525–4529.

Kessler, H., Loosli, H. R., & Oschkinat, H. (1985) *Helv. Chim. Acta 68*, 661–681.

Kessler, H., Köck, M., Wein, T., & Gehrke, M. (1990) *Helv. Chim. Acta 73*, 1818–1832.

Kobel, H., & Traber, R. (1982) *Eur. J. Appl. Microbiol. Biotechnol. 14*, 237–240.

Koletsky, A. J., Harding, M. W., & Handschumacher, R. E. (1986) *J. Immunol. 137*, 1054–1059.

Krönke, M., Leonard, W. J., Depper, J. M., Arya, S. K., Wong-Staal, F., Gallo, R. C., Waldmann, T. A., & Greene, W. C. (1984) *Proc. Natl. Acad. Sci. U.S.A. 81*, 5214–5218.

Loosli, H. R., Kessler, H., Oschkinat, H., Weber, H. P., Petcher, T. J., & Widmer, A. (1985) *Helv. Chim. Acta 68*, 682–704.

Messerle, B. A., Wider, G., Otting, G., Weber, C., & Wüthrich, K. (1989) *J. Magn. Reson. 85*, 608–613.

Momany, F. A., McGuire, R. F., Burgess, A. W., & Scheraga, H. A. (1975) *J. Phys. Chem. 79*, 2361–2381.

Nemethy, G., Pottle, M. S., & Scheraga, H. A. (1983) *J. Phys. Chem. 87*, 1883–1887.

Neri, D., Szyperski, T., Otting, G., Senn, H., & Wüthrich, K. (1989) *Biochemistry 28*, 7510–7516.

Neri, D., Otting, G., & Wüthrich, K. (1990) *J. Am. Chem. Soc. 112*, 3663–3665.

Otting, G., & Wüthrich, K. (1988) *J. Magn. Reson. 76*, 569–574.

Otting, G., & Wüthrich, K. (1989) *J. Magn. Reson. 85*, 586–594.

Otting, G., & Wüthrich, K. (1990) *Q. Rev. Biophys. 23*, 39–96.

Otting, G., Senn, H., Wagner, G., & Wüthrich, K. (1986) *J. Magn. Reson. 70*, 500–505.

Quesniaux, V. F. J., Wenger, R. M., Schreier, M. H., & Van Regenmortel, M. H. V. (1987a) *Protides Biol. Fluids 35*, 507–510.

Quesniaux, V. F. J., Schreier, M. H., Wenger, R. M. Hiestand, P. C., Harding, M. R., & Van Regenmortel, M. H. V. (1987b) *Eur. J. Immunol. 17*, 1359–1365.

Quesniaux, V. F. J., Wenger, R. M., Schmitter, D., & Van Regenmortel, M. H. V. (1988) *Int. J. Pept. Protein Res. 31*, 173–185.

Sanner, M., Widmer, A., Senn, H., & Braun, W. (1989) *J. Comput. Aided Mol. Des. 3*, 195-210.
Schaumann, T., Braun, W., & Wüthrich, K. (1990) *Biopolymers 29*, 679-694.
Senn, H., Werner, B., Messerle, B. A., Weber, C., Traber, R., & Wüthrich, K. (1989) *FEBS Lett. 249*, 113-118.
Senn, H., Loosli, H. R., Sanner, M., & Braun, W. (1990) *Biopolymer 29*, 1387-1400.
Takahashi, N., Hayano, T., & Suzuki, M. (1989) *Nature 337*, 437-475.
Wider, G., Weber, C., Widmer, H., Traber, H., & Wüthrich, K. (1990) *J. Am. Chem. Soc. 112*, 9015-9017.
Wider, G., Weber, C., & Wüthrich, K. (1991) *J. Am. Chem. Soc.* (in press).
Wüthrich, K. (1976) *NMR in Biological Research: Peptides and Proteins*, North Holland/American Elsevier, New York.
Wüthrich, K. (1986) *NMR of Proteins and Nucleic Acids*, Wiley, New York.
Wüthrich, K. (1989) *Science 243*, 45-50.
Wüthrich, K., Wider, G., Wagner, G., & Braun, W. (1982) *J. Mol. Biol. 155*, 311-319.
Wüthrich, K., Billeter, M., & Braun, W. (1983) *J. Mol. Biol. 169*, 949-961.

# NMR Studies of [U-$^{13}$C]Cyclosporin A Bound to Cyclophilin: Bound Conformation and Portions of Cyclosporin Involved in Binding

S. W. Fesik,* R. T. Gampe, Jr., H. L. Eaton, G. Gemmecker, E. T. Olejniczak, P. Neri, T. F. Holzman, D. A. Egan, R. Edalji, R. Simmer, R. Helfrich, J. Hochlowski, and M. Jackson
*Pharmaceutical Discovery Division, Abbott Laboratories, Abbott Park, Illinois 60064*
*Received January 8, 1991; Revised Manuscript Received April 1, 1991*

ABSTRACT: Cyclosporin A (CsA), a potent immunosuppressant, is known to bind with high specificity to cyclophilin (CyP), a 17.7 kDa protein with peptidyl-prolyl isomerase activity. In order to investigate the three-dimensional structure of the CsA/CyP complex, we have applied a variety of multidimensional NMR methods in the study of uniformly $^{13}$C-labeled CsA bound to cyclophilin. The $^{1}$H and $^{13}$C NMR signals of cyclosporin A in the bound state have been assigned, and, from a quantitative interpretation of the 3D NOE data, the bound conformation of CsA has been determined. Three-dimensional structures of CsA calculated from the NOE data by using a distance geometry/simulated annealing protocol were found to be very different from previously determined crystalline and solution conformations of uncomplexed CsA. In addition, from CsA/CyP NOEs, the portions of CsA that interact with cyclophilin were identified. For the most part, those CsA residues with NOEs to cyclophilin were the same residues important for cyclophilin binding and immunosuppressive activity as determined from structure/activity relationships. The structural information derived in this study together with the known structure/activity relationships for CsA analogues may prove useful in the design of improved immunosuppressants. Moreover, the approach that is described for obtaining the structural information is widely applicable to the study of small molecule/large molecule interactions.

Cyclophilin (CyP)[1] is a 17.7 kDa protein (163 residues) that specifically binds to cyclosporin A (CsA; Figure 1), an immunosuppressive drug widely used in organ transplantation (Handschumacher et al., 1984). Although some exceptions have been noted (e.g., MeAla$^{6}$ CsA) (Durette et al., 1988), the relative affinity for cyclophilin within a series of cyclosporin A analogues correlates with their immunosuppressive activities (Handschumacher et al., 1984; Quesniaux et al., 1987, 1988; Durette et al., 1988). Thus, it has been hypothesized that the immunosuppressive activity of CsA is in some way mediated by binding to cyclophilin. The relationship between the binding of cyclosporin A to cyclophilin and the inhibition of T-cell activation at the molecular level is still unresolved. However, it has been suggested that some of the biological effects of CsA (Takahashi et al., 1989) may be linked to the inhibition of the cyclophilin-catalyzed cis-trans isomerization of peptide bonds involving proline (Takahashi et al., 1989; Fischer et al., 1989). As shown for another immunosuppressant (FK506) that binds to a different peptidyl-prolyl cis-trans isomerase, however, isomerase inhibition may not be the only requirement for immunosuppressive activity (Bierer et al., 1990).

In order to aid in the design of CsA analogues that are clinically useful as immunosuppressants, it would be of value to determine the bound conformation of CsA and to identify those portions of CsA that bind to CyP. The CsA analogues synthesized to date (Wenger, 1983, 1985; Durette et al., 1988;

* To whom correspondence should be addressed.

[1] Abbreviations: CyP, cyclophilin; CsA, cyclosporin A; NMR, nuclear magnetic resonance; ATCC, American type culture collection; HMQC, heteronuclear multiple-quantum correlation; TOCSY-REVINEPT, total correlation spectroscopy-reverse insensitive nucleus enhancement by polarization transfer; DIPSI, decoupling in the presence of scalar interactions; GARP, globally optimized alternating-phase rectangular pulses; NOE, nuclear Overhauser effect; COSY, correlation spectroscopy; HMBC, heteronuclear multiple-bond correlation; AMT, American Microwave Technologies; TTL, transistor transistor logic; HSQC, heteronuclear single-quantum correlation; HMQC-NOESY, heteronuclear multiple quantum correlation-nuclear Overhauser effect spectroscopy; TPPI, time-proportional phase incrementation; PTS, programmed test sources; MeAla, *N*-methylalanine; MeVal; *N*-methylvaline; MeBmt, (4*R*)-*N*-methyl-4-butenyl-4-methylthreonine; Abu, aminobutyric acid; Sar, sarcosine; MeLeu, *N*-methylleucine; MePhe, *N*-methylphenylalanine; MeIle, *N*-methylisoleucine; MeThr, *N*-methylthreonine.

0006-2960/91/0430-6574$02.50/0 